





Optimized scheme for paired transverse corrective forces in S-shaped scoliosis via ultrasound and application in Chêneau brace: a pilot study

Li Wang¹, Nan Xia¹ , Chun Wang^{1,2}, Qian Zheng¹, Christina Zonghao Ma³ , Ahmed S. A. Youssef^{1,4} , Chao Zhang⁵, Youbin Deng⁵, Guoli Zhu⁶ and Xiaolin Huang¹ 

Abstract

Background: There is currently no consensus on the optimal positions of the transverse corrective forces (TCFs) for scoliosis braces.

Objectives: This study aimed to explore an optimal scheme of placing paired TCF for S-shaped adolescent idiopathic scoliosis and its feasibility in Chêneau brace (CB) treatment.

Study design: Cross-over feasibility pilot trial.

Methods: Ten S-shaped adolescent idiopathic scoliosis participants were invited to receive four tests with different paired TCF positions under ultrasound. The positions of the paired TCF were test 1: thoracic apical vertebra (AV), lumbar AV; test 2: 2 cm inferior to thoracic AV, lumbar AV; test 3: thoracic AV, 2 cm superior to lumbar AV; and test 4: 2 cm inferior to thoracic AV, 2 cm superior to lumbar AV. The test scheme with the highest mean in-force correction rate (IFCR) for the thoracic spinous process angle (SPA) was further applied in the CB fabrication of 4 additional participants.

Results: A significant higher mean IFCR of the thoracic SPA of 63.6% was found in test 2 ($P < 0.001$), which also contributed to its higher overall IFCR of the SPA of 64.6% ($P = 0.001$). Moreover, the mean in-brace correction rates for the thoracic and overall curves in CB were 46.4% and 51.8%, respectively. No adverse events were reported.

Conclusions: Placing paired TCF at the lumbar AV and 2 cm inferior to the thoracic AV achieved better treatment efficacy than other schemes. The practical application of this scheme on the CB was feasible.

Keywords

adolescent idiopathic scoliosis, transverse corrective force, Chêneau brace, ultrasound, Cobb angle

Date received: 15 February 2021; accepted 15 September 2021.

Introduction

Adolescent idiopathic scoliosis (AIS) is defined as an unexplained lateral spine curvature accompanied by rotation that occurs in teenagers, with a prevalence rate of 2%–3%.¹ AIS is progressive and may be associated with adverse health outcomes (e.g. back pain² and pulmonary dysfunction³). Therefore, early effective treatments are needed to stop the progression and improve the quality of life.

Spinal orthosis or spinal brace is a traditional rehabilitation treatment for patients with moderate AIS. High-quality evidence has confirmed its efficacy in restoring scoliosis or preventing the progression of scoliosis.^{1,4} Among different designs of spinal braces, the “Chêneau brace” (CB) has been the most commonly prescribed in AIS patients in Europe and mainland China.⁵ CB and its derivatives are anterior opening asymmetric thoraco-lumbar-sacral orthoses with expansion voids at the concavities. Emphasizing

¹Department of Rehabilitation Medicine, Tongji Hospital, Tongji Medical College, Huazhong University of Science and Technology, Wuhan, China

²Department of Rehabilitation Medicine, Shantou Central Hospital, Shantou, China

³Department of Biomedical Engineering, the Hong Kong Polytechnic University, Hong Kong SAR, China

⁴Basic Science Department, Faculty of Physical Therapy, Beni-Suef University, Beni-Suef, Egypt

⁵Department of Medical Ultrasound, Tongji Hospital, Tongji Medical College, Huazhong University of Science and Technology, Wuhan, China

⁶School of Mechanical Science and Engineering, Huazhong University of Science and Technology, Wuhan, China

Corresponding author:

Xiaolin Huang, Department of Rehabilitation Medicine, Tongji Hospital, Tongji Medical College, Huazhong University of Science and Technology, 1095 Jiefang Avenue, Wuhan 430030, China. Email: xiaolin2006@126.com

Associate Editor: Nachiappan Chockalingam

“X.L.H. et al., “X.L.H., L.W., N.X., C.W., Z.Q., C.Z.M., A.S.A.Y., C.Z., Y.B.D., and G.L.Z., designed the study; X.L.H., L.W., et al, carried out the work. All authors contributed to the manuscript preparation.” See in the author contribution section. “It is important to acknowledge that the team of Y.D. provided the technology of three dimensional spinal ultrasound and the team of G.Z. helped us develop the Pneumatic Bracing Simulation System.” See in the acknowledgments section. “Optimized scheme for paired transverse corrective forces in S-shaped scoliosis via ultrasound and application in Chêneau brace: a pilot study.

Copyright © 2021 The Authors. This is an open access article distributed under the terms of the Creative Commons Attribution-Non Commercial-No Derivatives License 4.0 (CCBY-NC-ND), where it is permissible to download and share the work provided it is properly cited. The work cannot be changed in any way or used commercially without permission from the journal.

DOI: 10.1097/PXR.000000000000064

three-dimensional (3D) correction of the spinal deformity, CB can work synergistically with physiotherapeutic scoliosis-specific exercises to optimize the overall treatment effect.⁵ However, the current design and fabrication processes for CB rely heavily on the personal experience of orthotists, which directly determines the success or failure of brace treatment.⁶

Both transverse corrective forces (TCFs) and axial traction forces are applied for the correction of coronal deformity in scoliosis.⁷ However, the former are more efficient than the latter for scoliosis with Cobb angles less than 53 degrees.⁷ Therefore, TCFs are more crucial in brace treatment (mainly prescribed in patients with Cobb angles 20–40 degrees).^{4,8} However, orthotists have not yet reached a consensus on the proper positions of paired TCFs for both thoracic and lumbar curves in scoliosis.⁹ In a survey, half the experts recommended locating the TCF at the level of the apical vertebra (AV) for the thoracic curve, whereas the other half recommended the apical rib.⁹ An early study of model analysis suggested that the appropriate positions of TCFs for the thoracic and lumbar curves were at the apical rib and at (or superior to) the apex, respectively.¹⁰ However, Karam et al.¹¹ provided a different opinion from his observation of better reduction for thoracic deformity when applying a lateral force at the level of the AV instead of apical rib. In addition, the corrective effect of two opposing TCFs acting on adjacent spine segments of curvatures will affect each other¹²; thus, the position selection of the paired TCFs for the thoracic and lumbar curves in S-shaped scoliosis is more complicated. Locating the TCFs in the fabrication process of braces for S-shaped scoliosis becomes an issue that needs to be addressed.

Recently, spinal ultrasound technology has gradually been used to aid the fabrication of braces. Li et al.¹³ found a better in-brace correction effect of braces made through ultrasound evaluation compared with conventional production processes. In his study, brace fabrication was optimized through the corrective effect test with different positions of pressure pads. Subsequent research further affirmed the role of ultrasound evaluation in optimizing the magnitude and position of the corrective forces in brace fabrication.¹⁴ Although these studies proved the function of ultrasound in optimizing brace design, generally applicable schemes of pressure positions for AIS have not been reported.

To address the abovementioned issues, this study aimed to investigate the relationship between the positions of paired TCFs and the corrective effect in scoliosis braces and answer the research questions of where to locate the paired TCFs. We hypothesize that there is likely to be a common optimal position scheme of paired TCFs for the brace of S-shaped scoliosis. Therefore, in this study, we compared the corrective effects of the four tests with different position combinations in S-shaped AIS under ultrasound and selected the optimal scheme to validate its feasibility in CB treatment.

Materials and methods

Participants

The inclusion criteria for participants were as follows: (1) age of 10–16 years; (2) a diagnosis of idiopathic scoliosis with a primary Cobb angle between 20 and 50 degrees; (3) S-shaped curves (right thoracic and left lumbar curves); (4) Risser sign of 0–4; (5) body

mass index ≤ 25 kg/m²; and (6) agreement to sign the informed consent form. In addition, participants were further classified according to the Peking Union Medical College (PUMC) classification.¹⁵ Since patients with severe scoliosis insisted on brace treatment and may benefit from it,¹⁶ the inclusion criteria of the maximum Cobb angle in our study were slightly enlarged compared with the standardized criteria proposed by the Scoliosis Research Society.⁸ The exclusion criteria were as follows: (1) suffering from spinal-related diseases, such as lumbar disc herniation and spinal tuberculosis; (2) suffering from pressure-intolerant diseases, such as local skin ulcers, etc.; (3) a history of spinal surgery; and (4) a history of scoliosis treatment involving surgery, brace, exercise, etc.

Ten AIS participants were invited to explore the optimal scheme for paired positions of TCFs in S-shaped AIS by ultrasound in the first part of the study. Four additional participants were recruited to study the feasibility of applying the optimal scheme to the fabrication of CB in the second part of the study.

The research protocol was approved by the Ethical Committee of the Tongji Medical College, Huazhong University of Science and Technology (certificate of approval number 2020-S257). The research was prospectively registered at Chinese clinical trial registry (registration number: ChiCTR2000040757). Informed consent was obtained from all participants and their legal guardians.

Pneumatic bracing simulation system

A pneumatic bracing simulation system (Figure 1) was developed to simulate the classic three-point corrective forces system of CB referring to the Providence brace system¹⁴ and Fixation, Elongation, Derotation system.¹⁷ In a cuboid frame, a pair of underarm pallets and pelvic baffles were designed to fix both arms and the pelvis. A passive fixed pushrod and a pair of pneumatic pushrods driven with air cylinders (MDWBF40–400, SMC, Japanese) constitute the paired TCFs output. C-shaped curved pads (20*4*2 cm) with certain elasticity are placed innermost of these pushrods. The C-shaped curved pad is composed of an iron plate, a cushion (NORA Lunairmed 0.6 cm, ethylene-vinyl acetate thermoplastic materials), and a black cloth. The height and horizontal displacement of the pushrods can be adjusted appropriately to meet the needs of participants. The pneumatic pushrod can stretch out or draw back and apply a constant corrective force to the torso. The magnitude of the paired TCFs and the safety of the system are controlled by a closed-loop pneumatic control system, which is assembled mainly with a preprogrammed controller (STM32-P01, ST, China). The overall pneumatic control system diagram is shown in Figure 2. The stability of the power output and operational safety of the equipment passed our pretest.

Clinical procedure

In a quiet warm room, the participants were first asked to remove upper garments and wear a back-opening gown. They were then instructed to sit in the center of the seat without gaps between the pelvic baffles and the thighs, keeping the hips and knees bent at 90 degrees and the line connecting the spinous processes of C7 and S2 perpendicular to the seat. Their upper limbs were placed on the underarm pallets, with shoulder abduction 90 degrees, elbow flexion 90 degrees, and neutral forearm positioning. After the above posture preparation, the body positions of AVs were located and marked by an experienced therapist through surface palpation referring to the

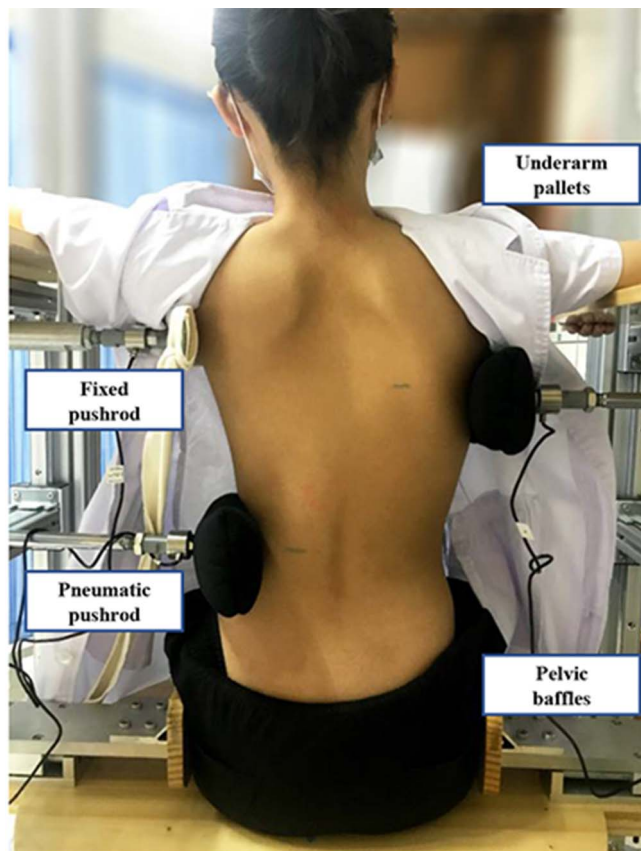


Figure 1. Pneumatic bracing simulation system.

full-spine standing x-ray taken in the last month. The heights from the seat surface to each AV level were recorded accordingly.

Referring to previous research by Li et al,¹⁸ the prescribed TCFs points at the AV level and 2 cm up/down were all involved in our study. Considering that the application of TCF at 2 cm superior to the thoracic AV and 2 cm inferior to the lumbar AV will cause obvious discomfort to the armpits and iliac crest, we discarded

those two points. Because excessively lower position of the TCF of the thoracic curve may hinder the correction of the lumbar curve,¹² we chose the position of 2 cm inferior to the AV instead of more inferior position. Thus, there were four possible combinations for the entire study: test 1 (thoracic AV, lumbar AV), test 2 (2 cm inferior to thoracic AV, lumbar AV), test 3 (thoracic AV, 2 cm superior to lumbar AV), and test 4 (2 cm inferior to thoracic AV, 2 cm superior to lumbar AV). Each participant received the four tests in random order. Referring to our pretest and study by Chen et al,¹⁹ the participants received a pair of TCFs provided by pneumatic bracing simulation system, setting at 25% of the weight of the participants for 30 continuous seconds for each test. An interval of 30 minutes was set between each pair of tests to eliminate the reserved effect from the last test. During the intervals, participants were permitted to sit quietly or perform some daily activities under the supervision of the doctor, and exercise training (such as stretch) was forbidden. The corrective effects of the four tests were evaluated by ultrasound.

Ultrasound evaluation

All ultrasound examinations were performed by one experienced expert with a GE LOGIQ e9 Ultrasound machine (GE Healthcare, Chicago, IL). The ultrasound machine was equipped with a sensor-based electromagnetic navigation system, a C2–6 convex array transducer, and a paired 3D magnetic position sensor provided by the same factory, which can be attached to the transducer to determine the orientation and position of the transducer (Figure 3). The commercial ultrasound machine showed good reliability and validity in evaluating scoliosis.²⁰ Before formal ultrasound scanning, the following preparations were needed. First, the position of the electromagnetic navigation system was adjusted to ensure that the participant’s spine was located in the 60 degrees sector-shaped region with a diameter of 1 m in front of the center of the navigation system. Second, the participant’s spine was prescanned from C7–S1 to ensure that ultrasound signal reception was good (the green indicator light indicates a good signal) throughout the whole scanning process. Finally, the frequency of the transducer was set at 6 MHz, the scanning depth at 7 cm, the gain at 66 dB, and the time gain compensation at general settings.

Each participant was scanned at baseline and at the end of each test five times. After scanning, the built-in ultrasound software program was used for 3D image construction. Images that can clearly show the structure of the spinous process and transverse process or lamina on the coronal plane and the horizontal plane were manually obtained from the 3D image and saved as pictures. The spinous process angle (SPA) on the coronal plane and the lamina method of axial vertebral rotation (AVR) angle on the horizontal plane were measured with ImageJ 1.52a software by a doctor who was not involved in these tests. The SPA was explained as the angle between the most tilted spinous process line (between two spinous processes) of the upper area of the curve and the most tilted spinous process line of the lower area.²¹ The AVR angle (lamina method) was determined as the angle between the laminae line (line between center of the right and left laminae) and the horizontal reference line.²² The specific image acquisition and angle measurement process of SPA and AVR are shown in Figure 4. The test scheme with the highest correction rate of thoracic SPA

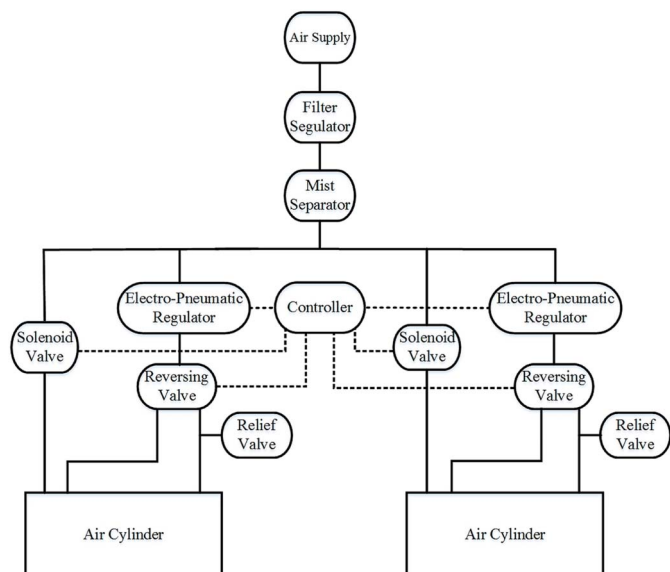


Figure 2. Pneumatic control system diagram.

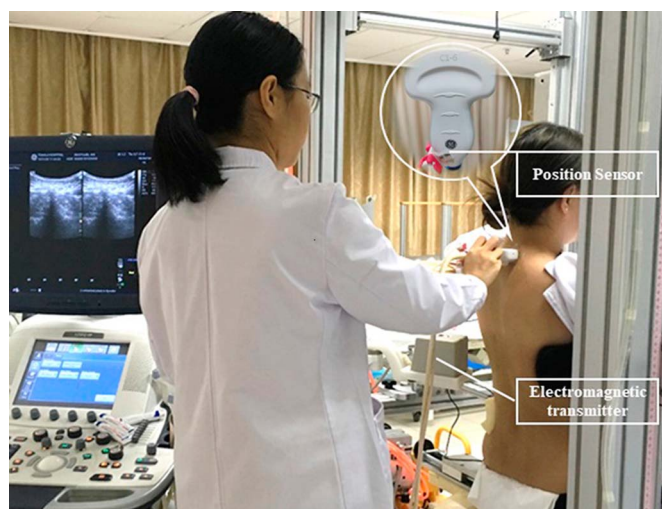


Figure 3. Ultrasound imaging system.

was adopted to further explore the feasibility of the application in CB treatment.

CB fabrication and evaluation

CBs were designed and fabricated for the other four S-shaped new AIS recruits using the selected scheme summarized from the previous exploration. First, an experienced orthotist was invited to mark the AVs of the curves in the body with a special marker pen. Second, a positive mold of the participant's upper torso was obtained. Then, the selected TCF positions (pressure centers) and their corresponding pressure zones were duplicated on the positive mold. Next, the thickness of the plaster in the target pressure zones and other necessary operations on the existing model were adjusted. Finally, after vacuuming, cutting, and grinding, the original CB was formed. The participants were then invited to

perform a continuous 2-hour wearing test, and the skin turned red in areas with relatively higher pressure. When the participants took off the braces, the immediate pressure zone (red area) on the skin was recorded and measured through the Global Posture System (Chinesport, Italy),²³ which is a computerized photographic postural assessment system. If the recorded pressure zones were inconsistent with the target pressure zones, the inner surface of the target pressure zones on CB were pasted with soft cushions to achieve the desired pressure zone design.

After the CBs were checked with no problems, the participants were first instructed to gradually increase the brace wearing time to more than 20 hours per day within 1 week according to their tolerance. Then, they were asked to wear the braces for more than 20 hours per day in the following 1 week. The participants and their parents were asked to record the daily wear time in a diary and provide feedback through the WeChat app. The orthotist checked the feedback from the diary and WeChat at the follow-up. After 2 weeks of qualified brace treatment, a full-spine x-ray was taken while the participant was wearing the CB. Details of the fabrication process of CB are shown (see Table, Supplemental Digital Content 1, <http://links.lww.com/POI/A65>, which demonstrates more details about the special fabrication process of the CB).

Data collection

Demographic characteristics, full-spine standing radiographs, and medical history were collected for each participant. The primary outcomes were the in-force correction rate (IFCR) of SPA for each thoracic or lumbar curve and the overall IFCR of SPA for the two curves together from ultrasound. The IFCR of SPA was calculated as follows: $\text{SPA-IFCR}\% = (\text{baseline SPA} - \text{in-force SPA}) / \text{baseline SPA} * 100\%$. The overall IFCR represents the average of the two IFCRs of corresponding thoracic and lumbar curves for each

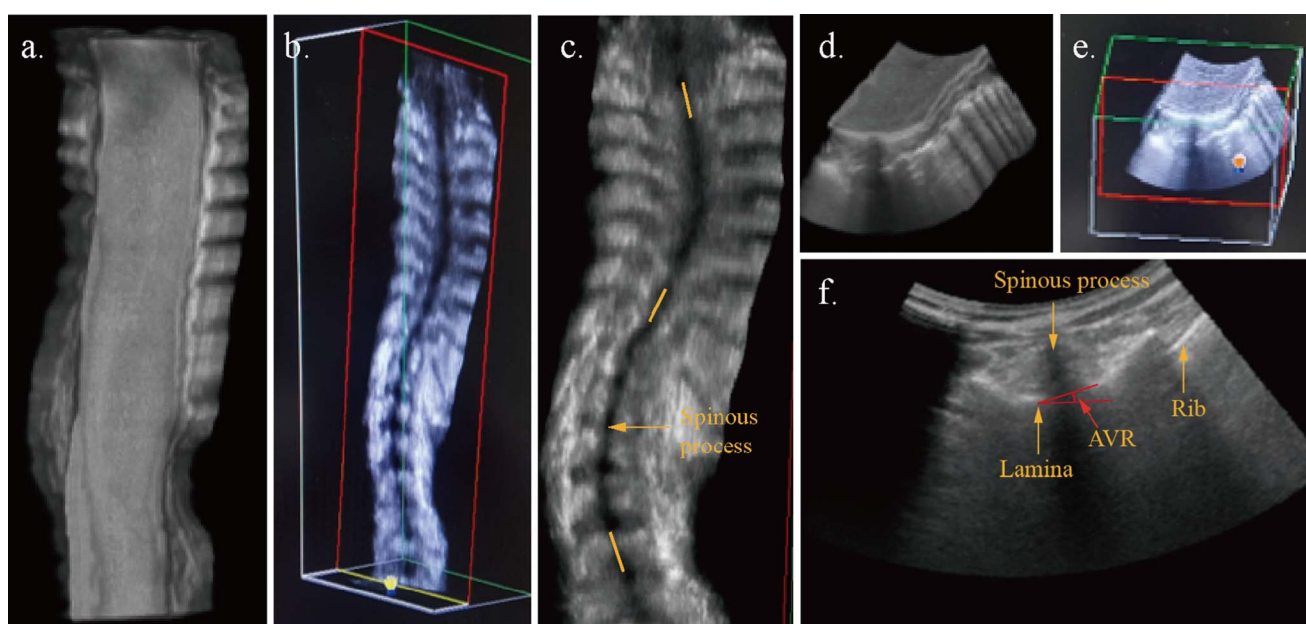


Figure 4. (a) Coronal image of the raw 3D spinal ultrasound; (b) acquisition of a coronal image with clear spinous processes; (c) measurement of the SPA (yellow lines are the most tilted lines between two spinous processes); (d) horizontal image of the raw 3D spinal ultrasound; (e) acquisition of a horizontal image with clear apical vertebra; (f) measurement of the AVR (red line below is the horizontal reference line). 3D = three-dimensional.

Table 1. Baseline characteristics of participants in the first part.

No	Age (y)	Sex	Height (cm)	BMI (kg/m ²)	Risser sign	T/L Cobb angle (degrees)	T/L rotation (degrees)	T/L AV
1	15	F	161	21.2	3	33/30	16/12	T8/L2
2	12	F	162	15.6	2	22/15	6/6	T9/L2
3	13	F	150	13.8	3	22/23	8/18	T8/L2
4	12	F	150	15.6	3	38/40	8/18	T7/L1
5	13	F	160	16.4	3	35/47	8/24	T8/L2
6	16	M	175	18.3	4	18/30	4/28	T8/L1
7	12	F	166	17.4	0	35/22	16/2	T8/L2
8	15	F	165	22.0	4	39/37	6/16	T7/L1
9	15	F	172	14.9	3	28/30	26/10	T7/L2
10	16	M	175	17.6	4	28/25	10/14	T8/L1
Mean (SD)	13.9 (1.7)	/	163.6 (9.0)	17.3 (2.6)	2.9 (1.2)	29.8(7.3)/29.9(9.4)	10.8(6.7)/14.8(7.8)	/

Abbreviations: AV, apical vertebra; BMI, body mass index; L, lumbar; T, thoracic.

participant. The secondary outcomes were the IFCR of AVR in the ultrasound tests for thoracic or lumbar curves and the overall IFCR, which were calculated using the same methods above. Moreover, the in-brace correction rate (IBCR) of the Cobb angle and the Raimondi AVR angle were also measured through the same methods above. The adverse events were recorded in detail simultaneously.

Statistical analyses

All statistical analyses were completed using IBM SPSS Statistics 22 software (IBM, Armonk, NY). Normality of the data was assessed by using the Shapiro–Wilk test. Repeated-measures analyses of variance with additional Bonferroni-corrected post hoc multiple comparisons were used to compare measurement differences of the four tests. The Greenhouse–Geisser correction was performed when the sphericity assumption was violated. The threshold for significance was taken as $P < 0.05$.

Results

In the first part of the study, 10 S-shaped AIS participants with a mean age of 13.9 ± 1.7 years were included. The median Risser sign index was three, with an interquartile range of one. The mean

Cobb angles/Raimondi AVR angles of the thoracic and lumbar curves were 29.8/10.8 and 29.9/14.8 degrees, respectively. Seven participants were PUMC-IIb, one participant was PUMC IIc, and two participants were PUMC IId. More details of the demographics and baseline measurements of the participants are shown in Table 1.

The mean SPA angles of the thoracic and lumbar curves were 29.5 and 26.6 degrees, respectively. The mean thoracic and lumbar SPA-IFCRs of the four tests ranged from 38.5% to 63.6% and from 61.7% to 65.6%, respectively. The overall SPA-IFCRs from test 1 to test 4 were 52.4%, 64.6%, 50.8%, and 51.6%, respectively. Significant differences were detected in both the mean thoracic SPA-IFCR ($P < 0.001$) and the overall SPA-IFCR ($P = 0.001$) among the four tests, but no difference was detected in the mean lumbar SPA-IFCR ($P > 0.05$). Further pairwise comparison by post hoc test suggested that the mean thoracic SPA-IFCR in test 2 was significantly higher than the mean thoracic SPA-IFCR in the other tests ($P < 0.001$). Moreover, the overall SPA-IFCR in test 2 was significantly higher than the overall SPA-IFCR in test 1 ($P = 0.001$), test 3 ($P = 0.007$), and test 4 ($P = 0.004$). No differences were found in these indicators among the remaining three tests ($P > 0.05$).

The mean AVR angles of the thoracic and lumbar curves were 14.7 and 10.5 degrees, respectively. The mean thoracic and lumbar IFCRs of AVR angles of the four tests ranged from 15.9% to

Table 2. The IFCRs of SPA and AVR angle for thoracic, lumbar, and overall curves under four tests in the first part (N = 10).

By ultrasound	Test 1	Test 2	Test 3	Test 4
Mean IFCR (SD) of thoracic SPA (%)	41.4 (21.4) ^c	63.6 (21.3) ^a	38.5 (23.0) ^c	41.6 (30.2) ^c
Mean IFCR (SD) of lumbar SPA (%)	63.5 (20.4)	65.6 (20.0)	63.1 (20.0)	61.7 (23.9)
Overall IFCR (SD) of SPA (%)	52.4 (17.7) ^d	64.6 (17.7) ^b	50.8 (17.9) ^d	51.6 (22.2) ^d
Mean IFCR (SD) of thoracic AVR (%)	15.9 (11.1)	21.5 (16.4)	18.1 (7.3)	17.0 (11.4)
Mean IFCR (SD) of lumbar AVR (%)	30.0 (15.8)	26.8 (13.4)	33.9 (21.4)	31.3 (15.1)
Overall IFCR (SD) of AVR (%)	23.0 (12.5)	24.2 (10.5)	26.0 (12.7)	24.2 (11.4)

Abbreviations: AVR, axial vertebral rotation; IFCR, in-force correction rate; SPA, spinous process angle.

^a $P < 0.001$ among four tests.

^b $P < 0.01$ among four tests.

^c $P < 0.001$ compared with test 2.

^d $P < 0.01$ compared with test 2.

Table 3. The baseline characteristics, Cobb angles, AVR angles, and IBCRs in x-ray of participants in the second part.

No	Sex	Age (y)	Height (cm)	BMI (kg/m ²)	T/L AV	Baseline Cobb angle for T/L (degrees)	Baseline AVR angle for T/L (degrees)	IBCR of Cobb angle for T/L (%)	IBCR of AVR angle for T/L (%)
1	F	14	156	18.5	T9/L2	35/26	6/18	51.4/50.0	33.3/66.7
2	F	13	161	14.3	T9/L2	38/29	6/4	39.5/69.0	33.3/100
3	F	13	160	16.4	T8/L2	35/47	8/24	42.9/55.3	25.0/75.0
4	M	15	173	16.4	T9/L2	31/31	6/18	51.6/54.8	33.3/33.3
Mean (SD)	/	13.8 (1.0)	162.5 (7.3)	16.4 (1.7)	/	34.8(2.9)/33.3(9.4)	6.5 (1.0)/16.0(8.5)	46.4(6.1)/57.3(8.2)	31.2(4.2)/68.8(27.5)

Abbreviations: AV, apical vertebra; AVR, axial vertebral rotation; BMI, body mass index; IBCR, in-brace correction rate; L, lumbar; T, thoracic.

21.5% and from 26.8% to 33.9%, respectively. The overall IFCRs of AVR angles ranged from 23% to 26%, with the highest in test 3 at 26.0%. However, no differences were detected in the IFCR of AVR angles for thoracic, lumbar, and overall curves among the 4 tests ($P > 0.05$). The IFCRs of SPA and AVR angles in ultrasound of the four tests are shown in Table 2. The details of the ultrasound outcome for each participant in the first part are shown (see Table, Supplemental Digital Content 2, <http://links.lww.com/POI/A66>, which demonstrates more details about the ultrasound outcomes).

In the second part, four new S-shaped recruits were included as participants. The median Risser sign index was three, with an interquartile range of 0.5. The mean Cobb angles/AVR angles (Raimondi method)²⁴ of the thoracic and lumbar curves were 34.8/6.5 and 33.3/16.0 degrees, respectively. According to the results from the first part, the target TCF positions on the CB were designed at the AV of the lumbar curve and 2 cm inferior to the AV of the thoracic curve, respectively. The mean IBCRs of the Cobb angle/AVR angles for the thoracic and lumbar curves were 46.4%/31.2% and 57.3%/68.8%, respectively. The IBCRs of the Cobb angle and AVR angle for the overall curves were 51.8% and 50%, respectively. More details of the demographics and outcome measures are shown in Table 3. No adverse events occurred throughout the test procedure.

Discussion

This pilot study was the first attempt to explore the generic optimal scheme on the positions of TCFs for S-shaped scoliosis by comparing the correction rates of thoracolumbar deformity via ultrasound. Our preliminary results suggested that setting paired TCFs at the lumbar AV and 2 cm inferior to the thoracic AV achieved the best corrective effect for the thoracic curve and overall efficacy. The feasibility and effectiveness of this scheme were initially verified in the subsequent CB fabrication.

Our results demonstrated that the overall SPA-IFCR in test 2 was significantly better than the others, which was contributed by the mean SPA-IFCR of the thoracic curve. The reason for better results on mean SPA-IFCR for thoracic curve in test 2 than in test 1 and test 3 may be that appropriately lowering of the position of the TCF made the pressure pad closer to the apical rib level. Then, the transmission of TCF from the apical rib to the AV may be more effective than transmission directly from the muscles around the AV to the AV. In the design of the Boston brace system, one of the principles is placing the thoracic pad under the AV and the lumbar

pad at the AV,²⁵ which is matched with the optimal orthopedic force points found in our study. In addition, early modeling studies also confirmed that the force applied under the apex of the thoracic spine was better than the force applied at the apex.¹⁰ However, Karam et al¹¹ found that placing the orthotic force at the AV was more efficient than at the apical rib. Their results were different from our research mainly because different types of orthotic forces (a fulcrum force¹¹ vs. arc-shaped four-point pressure forces) were applied. In addition, different types of scoliosis and force positions may be also associated with different results. Moreover, we found that test 2 provided better results than test 4 even with the same TCF position for the thoracic curve, and the most likely cause of this difference can be attributed to the greater overlap and offset of the TCFs in test 4. However, no significant differences were found in the SPA-IFCRs for the lumbar curve among the four tests. Unlike the thoracic spine, the TCF was transmitted to the lumbar vertebra through soft tissue instead of the rib cage. Mechanical conduction through muscle and soft tissue may be more blurred. Future studies are needed to further explore how orthotic forces are transmitted from the body surface to the spine.

In the four tests, the SPA-IFCRs of the thoracic curve were slightly lower than the SPA-IFCRs of the lumbar curve, which was consistent with the study of Chen et al.¹⁹ The lower IFCR in the thoracic curve may be attributed to the reduced flexibility of the thoracic spine.²⁶ In addition, Thompson's study showed that thoracic curves were more prone to brace failure than lumbar curves.²⁷ Therefore, the correction of thoracic curves needs to be treated more carefully in the clinic. Moreover, the IBCR of Cobb angles reported in the literature was between 42% and 59%,²⁸⁻³⁰ which was lower than the overall SPA-IFCR of test 2 in our study, possibly because of the differences in the magnitude of the corrective force. The mean TCF output was 116 N in our study, which was relatively larger than the 10-73 N reported in braces.^{31,32} Thus, the optimal value of orthotic forces in braces should be explored to help achieve a better IBCR for both thoracic and lumbar curves in the future.

We also found that TCFs had an effect on decreasing the AVR and were more prominent in the lumbar region, which may be attributed mainly to the coupled motion of the spine. According to Fryette's laws, when the spine is neutral, side bending to one side will be accompanied by horizontal rotation to the opposite side.³³ Consequently, the correction of lateral bending was accompanied by the correction of rotation. Similarly, the lateral curvature of the lumbar curve decreased more than the lateral curvature of the

thoracic curve, so the vertebral rotation of the lumbar curve decreased more than the vertebral rotation of the thoracic curve. However, no significant differences were found in the AVR-IFCR among the four tests, possibly because the TCFs were applied only on the coronal plane, which created limited correction for rotation on the horizontal plane. In the future, we will further explore the appropriate derotation orthotic forces via ultrasound to improve the correction effect of vertebral rotation in the brace.

The second part of our research initially showed that it was feasible to apply the selected TCF scheme to the traditional manufacturing process of CB. The immediate IBCRs of the CB were reported to be between 42% and 59%,^{28–30} whereas the reported IBCR of the CB for the double major curve pattern was 50%.³⁰ In our study, the mean IBCRs of thoracic and lumbar curves were 46.4% and 57.3%, which exceeded the IBCR (from 40% to 50%) required by brace treatment.^{34,35} Thus, if the brace is worn in strict accordance with our order, the patient is likely to achieve a good correction for curves in the future.³⁴ Moreover, high-quality randomized control trials will be needed to further confirm the superiority of our scheme during brace fabrication or other applications.

Our study also had several limitations. First, the TCFs were applied only in the coronal plane in the first part. Honestly, to achieve better corrective effect for vertebral rotation, the application of oblique corrective forces may be better. However, because there is no uniform standard for the direction of the oblique corrective forces⁹ and the TCFs were the most critical forces for the correction of lateral curvature, TCFs instead of oblique corrective force were applied in our study. In the future, oblique corrective forces are needed to achieve the 3D correction of scoliosis. Second, the CBs were made by hand in the second part and the personal experience of the orthotist would inevitably affect the corrective effect of the CBs; thus, 3D printing is needed to reduce this limitation in the future. Finally, the relationship between the short-term and long-term bracing effects and the scheme of our ultrasound tests also needs further exploration.

Conclusions

Our study preliminarily demonstrated that placing the TCFs for lumbar and thoracic curves at the AV and at 2 cm inferior to the AV can bring more benefit to the correction of S-shaped scoliosis. The practical application of this scheme on CB was feasible.

Funding

The authors disclosed that they received no financial support for the research, authorship, and/or publication of this article.

Declaration of conflicting interest

The authors disclosed no potential conflicts of interest with respect to the research, authorship, and/or publication of this article.


Acknowledgments


The authors acknowledge the team of Professor Youbin Deng for providing the technology of three-dimensional spinal ultrasound


and the team of Professor Guoli Zhu for helping us develop the Pneumatic Bracing Simulation System.

ORCID iDs

N. Xia:  <https://orcid.org/0000-0002-9820-7127>

C.Z. Ma:  <https://orcid.org/0000-0001-6507-2329>

A.S.A. Youssef:  <https://orcid.org/0000-0003-3225-0189>

X. Huang:  <https://orcid.org/0000-0001-8618-9630>

Supplemental material

Supplemental material is available via direct URL citations in the HTML and PDF versions of this article on the website (www.POLjournal.org).

References

- Negrini S, Donzelli S, Aulisa AG, et al. 2016 SOSORT guidelines: orthopaedic and rehabilitation treatment of idiopathic scoliosis during growth. *Scoliosis Spinal Disord* 2018; 13: 3.
- Theroux J, Le May S, Hebert JJ, et al. Back pain prevalence is associated with curve-type and severity in adolescents with idiopathic scoliosis: a cross-sectional study. *Spine* 2017; 42: E914–E919.
- Yaszay B, Bastrom TP, Bartley CE, et al. The effects of the three-dimensional deformity of adolescent idiopathic scoliosis on pulmonary function. *Eur Spine J* 2017; 26: 1658–1664.
- Weinstein SL, Dolan LA, Wright JG, et al. Effects of bracing in adolescents with idiopathic scoliosis. *New Engl J Med* 2013; 369: 1512–1521.
- Kaelin AJ. Adolescent idiopathic scoliosis: indications for bracing and conservative treatments. *Ann Transl Med* 2020; 8: 28.
- Rigo M and Jelačić M. Brace technology thematic series: the 3D Rigo Chêneau-type brace. *Scoliosis Spinal Disord* 2017; 12: 10.
- White AA and Panjabi MM. The clinical biomechanics of scoliosis. *Clin Orthop Relat Res* 1976; 100–112.
- Richards BS, Bernstein RM, D'Amato CR, et al. Standardization of criteria for adolescent idiopathic scoliosis brace studies: SRS committee on bracing and nonoperative management. *Spine* 2005; 30: 2068–2075.
- Rigo M, Negrini S, Weiss HR, et al. “SOSORT consensus paper on brace action: TLSO biomechanics of correction (investigating the rationale for force vector selection)”. *Scoliosis* 2006; 1: 11.
- Andriacchi TP, Schultz AB, Belytschko TB, et al. Milwaukee brace correction of idiopathic scoliosis. A biomechanical analysis and a retrospective study. *J Bone Joint Surg Am* 1976; 58: 806–815.
- Karam JA, Eid R, Kreichati G, et al. Optimizing the vertical position of the brace thoracic pad: apical rib or apical vertebra? *Orthop Traumatol Surg Res* 2019; 105: 727–731.
- Wood G. Brace modifications that can result in improved curve correction in idiopathic scoliosis. *Scoliosis* 2014; 9: 2.
- Li M, Cheng J, Ying M, et al. Could clinical ultrasound improve the fitting of spinal orthosis for the patients with AIS? *Eur Spine J* 2012; 21: 1926–1935.
- Lou EH, Hill DL, Donauer A, et al. Results of ultrasound-assisted brace casting for adolescent idiopathic scoliosis. *Scoliosis Spinal Disord* 2017; 12: 23.
- Qiu G, Zhang J, Wang Y, et al. A new operative classification of idiopathic scoliosis: a peking union medical college method. *Spine* 2005; 30: 1419–1426.
- Lusini M, Donzelli S, Minnella S, et al. Brace treatment is effective in idiopathic scoliosis over 45°: An observational prospective cohort controlled study. *Spine J* 2014; 14: 1951–1956.
- Lapuente JP, Sastre S and Barrios C. Idiopathic scoliosis under 30 degrees in growing patients: a comparative study of the F.E.D. method and other conservative treatments. *Stud Health Technol Inf* 2002; 88: 258–269.
- Li M, Cheng J, Ying M, et al. Application of 3-D ultrasound in assisting the fitting procedure of spinal orthosis to patients with adolescent idiopathic scoliosis. *Stud Health Technol Inf* 2010; 158: 34–37.
- Chen ZQ, Wang CF, Bai YS, et al. Using precisely controlled bidirectional orthopedic forces to assess flexibility in adolescent idiopathic scoliosis: comparisons between push-traction film, supine side bending, suspension, and fulcrum bending film. *Spine* 2011; 36: 1679–1684.
- Lv P, Chen J, Dong L, et al. Evaluation of scoliosis with a commercially available ultrasound system. *J Ultras Med* 2020; 39: 29–36.

21. Brink RC, Wijdicks SPJ, Tromp IN, et al. A reliability and validity study for different coronal angles using ultrasound imaging in adolescent idiopathic scoliosis. *Spine J* 2018; 18: 979–985.
22. Chen W, Le LH and Lou EH. Reliability of the axial vertebral rotation measurements of adolescent idiopathic scoliosis using the center of lamina method on ultrasound images: in vitro and in vivo study. *Eur Spine J* 2016; 25: 3265–3273.
23. Yu QH, Huang HJ, Zhang Z, et al. The association between pelvic asymmetry and non-specific chronic low back pain as assessed by the global postural system. *BMC Musculoskelet Disord* 2020; 21: 596.
24. Weiss HR. Measurement of vertebral rotation: Perdriolle versus Raimondi. *Eur Spine J* 1995; 4: 34–38.
25. Wynne JH. The Boston Brace System philosophy, biomechanics, design & fit. *Stud Health Technol Inf* 2008; 135: 370–384.
26. van den Bogaart M, van Royen BJ, Haanstra TM, et al. Predictive factors for brace treatment outcome in adolescent idiopathic scoliosis: a best-evidence synthesis. *Eur Spine J* 2019;28: 511–525.
27. Thompson RM, Hubbard EW, Jo CH, et al. Brace success is related to curve type in patients with adolescent idiopathic scoliosis. *J Bone Joint Surg Am* 2017; 99: 923–928.
28. Lang C, Huang Z, Sui W, et al. Factors that influence in-brace correction in patients with adolescent idiopathic scoliosis. *World Neurosurg* 2019; 123: e597–e603.
29. Weiss HR, Tournavitis N, Seibel S, et al.. A prospective cohort study of AIS patients with 40° and more treated with a Gensingen Brace (GBW): preliminary results. *Open Orthop J.* 2017; 11: 1558–1567.
30. Weiss HR, Werkmann M and Stephan C. Correction effects of the ScolioLogiC “Chêneau light” brace in patients with scoliosis. *Scoliosis* 2007; 2: 2.
31. Karimi MT, Ebrahimi MH, Mohammadi A, et al. Evaluation of the influences of various force magnitudes and configurations on scoliotic curve correction using finite element analysis. *Australas Phys Eng Sci Med* 2017; 40: 231–236.
32. Périé D, Aubin CE, Petit Y, et al. Personalized biomechanical simulations of orthotic treatment in idiopathic scoliosis. *Clin Biomech* 2004; 19: 190–195.
33. Savarese RG, Capobianco JD and Cox JJ. *OMT Review: A Comprehensive Review in Osteopathic Medicine*. 3ed. Legis press New York, NY.; 2003.
34. Landauer F, Wimmer C and Behensky H. Estimating the final outcome of brace treatment for idiopathic thoracic scoliosis at 6-month follow-up. *Pediatr Rehabil* 2003; 6: 201–207.
35. Castro FP. Adolescent idiopathic scoliosis, bracing, and the Hueter-Volkman principle. *Spine J* 2003; 3: 180–185.